



OPEN

Changes in the negative logarithm of end-tidal hydrogen partial pressure indicate the variation of electrode potential in healthy Japanese subjects

Teruo Kiyama^{1,2,4}✉, Akira Tokunaga¹, Abumrad Naji³ & Adrian Barbul³

Molecular hydrogen (H₂) is produced by human colon microbiomes and exhaled. End-tidal H₂ sampling is a simple method of measuring alveolar H₂. The logarithm of the hydrogen ion (H⁺)/H₂ ratio suggests the electrode potential in the solution according to the Nernst equation. As pH is defined as the negative logarithm of the H⁺ concentration, pH₂ is defined as the negative logarithm of the H₂ effective pressure in this study. We investigated whether changes in pH₂ indicated the variation of electrode potential in the solution and whether changes in end-tidal pH₂ could be measured using a portable breath H₂ sensor. Changes in the electrode potential were proportional to (pH₂ - 2 × pH) in phosphate-buffered solution (pH = 7.1). End-tidal H₂ was measured in the morning (baseline) and at noon (after daily activities) in 149 healthy Japanese subjects using a handheld H₂ sensor. The median pH₂ at the baseline was 4.89, and it increased by 0.15 after daily activities. The variation of electrode potential was obtained by multiplying the pH₂ difference, which suggested approximately +4.6 mV oxidation after daily activities. These data suggested that changes in end-tidal pH₂ indicate the variation of electrode potential during daily activities in healthy human subjects.

Molecular hydrogen (H₂) is available in trace amounts in most ecosystems through atmospheric, biological, geochemical, and anthropogenic sources, and the atmosphere is critical for life as the main source of oxygen (O₂) for aerobic respiration¹. An obligately aerobic bacterium activates fermentative H₂ production to survive reductive stress during hypoxia². However, mammalian cells lack functional hydrogenase genes. H₂ metabolism in the human gut microbiome is driven by fermentative H₂ production and interspecies H₂ transfer³. In 2007, it was reported that 2–4% H₂ gas inhalation relieved brain ischemia–reperfusion injury in rats by selectively removing cytotoxic oxygen radicals⁴. H₂ released from intestinal bacteria can suppress inflammation induced in the liver by concanavalin A⁵. H₂ fermented by human microbiomes may affect aerobic metabolism under oxidative stress.

Stable aerobic and anaerobic states coexist in the lungs and colon of the human body. Intestinal gas contains up to 50% H₂ gas. Mucus H₂ concentrations were measured to be about 168 μM in the small intestines and 43 μM in the stomachs of live mice⁶. In general, biologically important gases behave like ideal gases; diffusion depends on the partial pressure gradient, but the dissolved gas concentration at equilibrium depends on both partial pressure and solubility. Although the alimentary tract is considered outside of the body, some of the H₂ generated in the colon is partly absorbed, passes in the circulating blood to the lungs, and diffuses into the alveolar space, where its presence can be easily determined⁷. However, after gas-exchange in the lungs, H₂ remains in arterial blood as well as the alveolar space according to Henry's law and distributes throughout tissues until saturation^{8,9}.

In plastic surgery, the H₂ clearance technique was introduced for monitoring postoperative blood flow after free-tissue transfer in a clinical study¹⁰. Briefly, H₂ is inhaled for 10–15 s and reaches the body tissue through arterial blood flow. Platinum electrodes are located in the tissue of interest. The generated electric current is proportional to the H₂ partial pressure in the tissue¹¹. The decay of H₂ concentration (clearance effect) is registered by the electrode. The mathematical analysis of clearance curves allows quantitative expression of blood flow value. In

¹Department of Gastrointestinal and Hepato-Biliary-Pancreatic Surgery, Nippon Medical School, Bunkyo, Tokyo, Japan. ²Department of Surgery, TMG Asaka Medical Center, Asaka, Saitama, Japan. ³Department of Surgery, Vanderbilt University School of Medicine, Nashville, TN, USA. ⁴Present address: Department of Surgery, Musashino Tokushukai Hospital, Nishi-Tokyo, Tokyo, Japan. ✉email: kiyama@nms.ac.jp

gastroenterology, an increase in the rate of breath H_2 excretion was introduced into clinical practice for the assessment of carbohydrate malabsorption and a simple method was used for measuring H_2 concentration in alveolar air by end expiratory sampling in the 1970s^{12,13}. The H_2 breath test has been widely used for diagnostic purposes in adults and children^{14,15}. Recently, an additional measurement of CH_4 concentration has been proposed to improve test accuracy¹⁶. These tests consist of an oral load with the corresponding sugar and the monitoring of the altered absorption by measuring the fermentation gases (H_2 and CH_4) in exhaled air. An increase in H_2 and/or CH_4 levels reflects the intestinal fermentation of non-absorbed sugars. In electrochemistry, the standard hydrogen electrode is an electrode for reference on all half-cell potential reactions and its standard electrode potential is declared to be 0 V at any temperature¹⁷. In aqueous solutions, the standard hydrogen electrode consists of a platinized Pt electrode and an acidic solution having a unit activity of proton (H^+) through which H_2 (gas) supplied at a fugacity of 1.00 bar is passed, ideally in the form of small bubbles so that the electrolyte solution quickly becomes saturated with the gas. The logarithm of the H^+/H_2 ratio reveals electrode potential in the solution according to the Nernst equation, while a negative logarithm of H^+ activity, which refers to the pH scale, is measured by a glass-electrode potential. Similarly, the H_2 exists at an effective pressure (known as the fugacity) in the gas state, while a hydrogen electrode potential is calculated by pH and the H_2 effective pressure.

The partial pressures of the separate dissolved gases are designated the same as the partial pressures in the gas state—that is, arterial partial pressure of O_2 (PaO_2) and arterial partial pressure of carbon dioxide ($PaCO_2$)¹⁸. Blood gases are mixed in vivo and not equilibrated. Although it is not practical to determine the mixed potential in vivo, the redox environment is considered as the summation of the products of the reduction potential and reducing the capacity of the linked redox couple¹⁹. O_2 is an oxidizing agent, and H_2 is an effective reducer. O_2 causes a rise of oxidation–reduction potential, and H_2 causes its reduction in the media of bacterial culture²⁰. However, the electrode potential represents the half-cell reaction under certain H_2 effective pressure against the standard hydrogen electrode ($E^0 = 0$)²¹. Therefore, it is practical to evaluate the difference between the two electrode potentials under different H_2 partial pressure wherever redox environment is common, while pH is measured by the difference between the two electrode potentials in the sample solution and the pH standard buffer solution²². Our hypothesis is that changes in the negative logarithm of H_2 effective pressure in the gas state will indicate variations of electrode potential in the solution, and those between before and after daily activities can be measured using a portable breath H_2 sensor in healthy Japanese subjects.

Results

Oxidation–reduction potential experiments. The H_2 electrode was based on the redox half-cell reaction: $2H^+(aq) + 2e^- \rightleftharpoons H_2(g)$. The electrode potential was calculated from the activity of H^+ and the fugacity of H_2 using the Nernst equation, as follows:

$$E = E_0 - \frac{RT}{2F} \ln \frac{f_{H_2}}{(a_{H^+})^2} = -\frac{2.303RT}{2F} \times \log \frac{f_{H_2}}{(a_{H^+})^2} \quad (V),$$

where a_{H^+} is the activity of H^+ , and f_{H_2} is the fugacity of H_2 , which, at low pressure, is equal to the ratio of the partial pressure of H_2 (P_{H_2}) over the standard pressure ($P^0 = 1 \text{ bar} = 10^5 \text{ Pa}$). pH is defined as $pH = -\log(a_{H^+})$. In this study, the pH_2 scale is defined as

$$pH_2 = -\log(f_{H_2}) = -\log\left(\frac{P_{H_2}}{P^0}\right)$$

The redox potential can be calculated from pH and pH_2 :

$$E_{H_2} = \frac{2.303RT}{2F} \times (pH_2 - 2pH) \quad (V)$$

The value of $2.303RT/2F$, the Nernst slope, was calculated at 22 °C, where R is the gas constant ($R = 8.314 \text{ J K}^{-1} \text{ mol}^{-1}$), T is the temperature ($T = 295.15 \text{ K}$), and F is the Faraday constant ($F = 9.6485 \times 10^4 \text{ C mol}^{-1}$); this equation yields results in mV, as follows:

$$2.303RT/2F = \frac{2.303 \times 8.314 \times 295.15}{2 \times 9.6485 \times 10^4} \times 10^3 = 29.3.$$

Changes in the oxidation–reduction potential (ORP) were measured after bubbling into a phosphate buffer solution of 100 parts per million (ppm) of standard H_2 gas and medical air to calculate the slope of $\Delta ORP / (pH_2 - 2 \times pH)$ at room temperature ($T = 22 \text{ }^\circ\text{C}$). The upper limit of pH_2 is 6.22, as yielded by 0.06 Pa- H_2 ($0.6 \times 10^{-6} \text{ bar}$) in medical air, and the lower calibration point of pH_2 is 4.0, as yielded by 10 Pa- H_2 standard gas ($1 \times 10^{-4} \text{ bar}$). In phosphate buffer solution ($pH = 7.1$), the ORP changed by $-56.7 \pm 17.0 \text{ mV}$ after bubbling of the standard H_2 gas and by a much lower degree ($+13.3 \pm 21.5 \text{ mV}$) after bubbling of the medical air ($p = 0.011$; Fig. 1).

The pH value after bubbling of the standard H_2 gas increased to 7.18 ± 0.03 in the phosphate-buffered solution compared to that of the medical air (7.08 ± 0.01 , $p = 0.0017$). The Nernst slope between H_2 partial pressures of 0.06 Pa and 10 Pa was calculated as

$$\text{Nernst Slope} = \frac{\Delta E_{H_2}}{\Delta(pH_2 - 2 \times pH)} = \frac{+13.3 - (-56.7)}{(6.2 - 2 \times 7.08) - (4.0 - 2 \times 7.18)} = 29.2$$

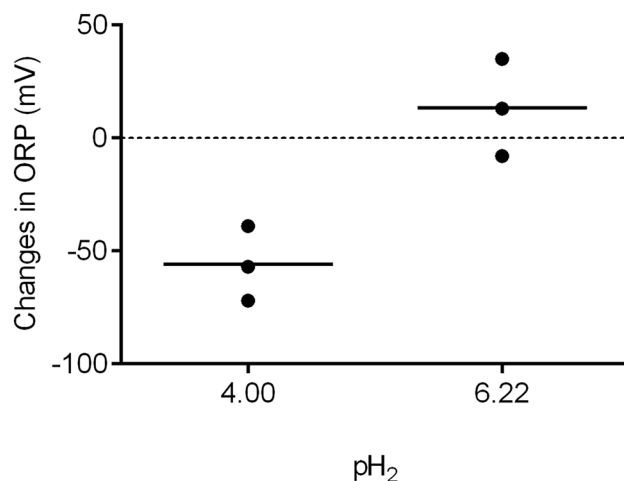


Figure 1. Changes in oxidation–reduction potential (ORP) in phosphate-buffered solution after bubbling air containing 10 Pa of H_2 ($pH_2=4.0$, $n=3$) and the atmosphere ($pH_2=6.22$, $n=3$) ($P=0.011$). $pH_2 = -\log\left(\frac{pH_2}{p^0}\right)$, $p^0 = 1 \text{ bar} = 10^5 \text{ Pa}$.

The measured $ORP/(pH_2 - 2 \times pH)$ slope agreed with the calculated Nernst slope ($2.303RT/2F$) under the low partial pressure of H_2 (0.06–10 Pa). The ORP was proportional to $(pH_2 - 2 \times pH)$ in the phosphate buffer solution.

Clinical study. The end-tidal H_2 is the level of H_2 released at the end of an exhaled breath. The end-tidal H_2 levels reflect the adequacy with which H_2 is carried in the blood back to the lungs and exhaled. The median end-tidal H_2 partial pressure at baseline was 1.3 Pa, varying within the range of 0.06 Pa (the atmospheric level) to 7.9 Pa (Table 1). Neither the timing of the most recent meal nor the timing of the most recent bowel movement had any influence on end-tidal H_2 measured at baseline.

The median end-tidal H_2 after daily activities was 0.9 Pa, which was significantly lower than the median value recorded at baseline ($P=0.007$, Fig. 2). Of all the subjects, 114 had eaten breakfast within 2 h of the baseline measurement, and no significant difference in H_2 partial pressure was observed between the values recorded at baseline and those recorded after daily activities. Before the baseline measurement in the morning, 74 subjects had had bowel movements, and no significant difference in H_2 partial pressure was observed between them.

The median pH_2 value was 4.89 at baseline, varying within the range of 4.10 to 6.22, and it increased to 5.05 after daily activities, varying within the range of 4.06 to 6.22 ($P=0.038$, Fig. 3, Table 2). A significant difference in the pH_2 value recorded between baseline and after daily activities was noted in the subjects who had not eaten breakfast (Fig. 4).

Discussion

The ORP of phosphate-buffered solution was changed according to the Nernst equation after air bubbling with and without low concentrations of H_2 and changes in ORP measured were proportional to $(pH_2 - 2 \times pH)$. In this study, the end-tidal H_2 decreased significantly from baseline to after daily activities, and the median pH_2

| Variables (n) | Baseline (Pa) | P [†] | After daily activities (Pa) | P [‡] |
|------------------------|---------------|----------------|-----------------------------|----------------|
| All (149) | 1.3 (0.5–2.6) | | 0.9 (0.4–1.9) | 0.007 |
| Gender | | | | |
| Male (51) | 1.4 (0.6–2.8) | 0.221 | 0.8 (0.4–1.9) | 0.045 |
| Female (98) | 1.1 (0.5–2.5) | | 1.0 (0.4–1.9) | 0.062 |
| Last meal | | | | |
| Breakfast (114) | 1.2 (0.5–2.6) | 0.197 | 1.0 (0.4–2.2) | 0.240 |
| Overnight fasting (35) | 1.6 (0.7–2.9) | | 0.7 (0.4–1.4) | 0.001 |
| Bowel movement | | | | |
| Yes (74) | 1.2 (0.5–2.3) | 0.252 | 0.8 (0.4–1.8) | 0.160 |
| No (75) | 1.4 (0.6–2.7) | | 1.0 (0.5–2.0) | 0.016 |

Table 1. Values of end-tidal H_2 at baseline and after daily activities in healthy Japanese subjects Data are presented as the median values (25th–75th percentile). [†]Male vs. female subjects, or yes vs. no. [‡]Baseline vs. after daily activities.

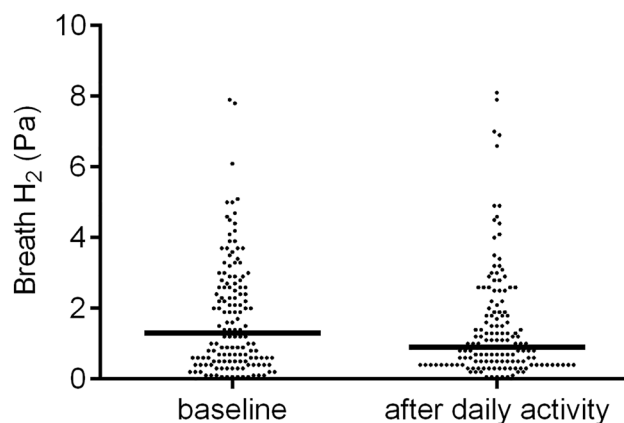


Figure 2. Breath hydrogen (H_2) partial-pressure measurements at baseline and after daily activities. Breath H_2 is end-tidal H_2 partial-pressure (Pa). The median end-tidal H_2 value of breath after daily activities was lower than the median value recorded at baseline ($P=0.007$).

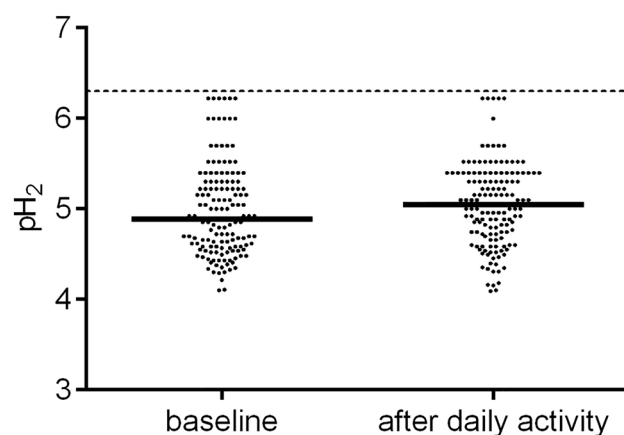


Figure 3. Values of pH_2 at baseline and after daily activities. The median value of pH_2 after daily activities was higher than that recorded at baseline ($P=0.038$).

| Variables (n) | Baseline | P^{\dagger} | After daily activities | P^{\ddagger} |
|------------------------|------------------|---------------|------------------------|----------------|
| All (149) | 4.89 (4.59–5.30) | | 5.05 (4.72–5.40) | 0.038 |
| Sex | | | | |
| Male (51) | 4.85 (4.55–5.22) | 0.221 | 5.10 (4.72–5.40) | 0.018 |
| Female (98) | 4.96 (4.60–5.30) | | 5.02 (4.72–5.40) | 0.367 |
| Last meal | | | | |
| Breakfast (114) | 4.92 (4.59–5.30) | 0.197 | 5.00 (4.64–5.40) | 0.605 |
| Overnight fasting (35) | 4.80 (4.54–5.15) | | 5.15 (4.85–5.40) | 0.001 |
| Bowel movement | | | | |
| Yes (74) | 4.92 (4.64–5.30) | 0.252 | 5.13 (4.74–5.40) | 0.488 |
| No (75) | 4.85 (4.57–5.22) | | 5.00 (4.70–5.30) | 0.023 |

Table 2. Values of pH_2 at baseline and after daily activities in healthy Japanese subjects. Data are presented as median (25th–75th percentile) values. † Male vs. female subjects or yes vs. no. ‡ Baseline vs. after daily activities.

at baseline was significantly lower than that after daily activities. However, the Nernst slope is proportional to temperature; thus, the Nernst slope ($2.303RT/2F$) = 30.8 at 37 °C (310.15 K). Because pH remains within the narrow normal range through acid–base homeostasis, the description of changes in electrode potential sidesteps the need to determine the pH value; $\Delta E \approx 30.8 \times [pH_2(\text{after daily activities}) - pH_2(\text{baseline})]$ (mV). After daily

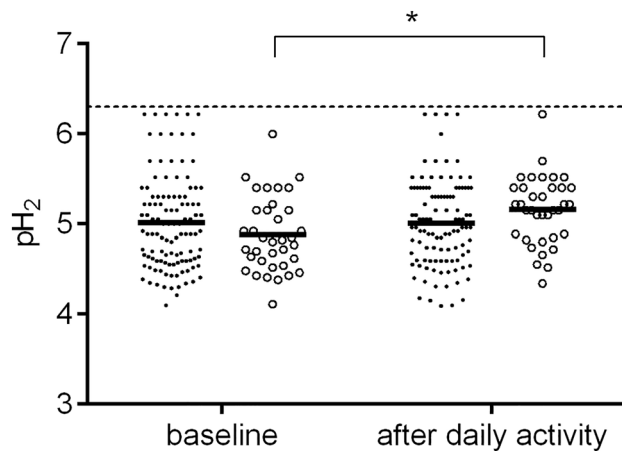


Figure 4. Values of pH_2 at baseline and after daily activities in the subjects with/without breakfast. The median value of pH_2 after daily activities was higher than that recorded at baseline in the subjects who had eaten breakfast * ($P=0.001$). The closed circle [●] indicates the subjects who had eaten breakfast and the open circle [○] indicates the subjects who had not eaten breakfast.

activities, pH_2 was found to increase to 0.15 over baseline in this study, and + 4.6 mV oxidation was estimated. It is suggested that changes in pH_2 indicate the variation of electrode potential due to alveolar air.

Excretion of H_2 in breath commonly persists despite an overnight fast. Although elevation of H_2 concentration above the fasting value after administration of a test sugar is evidence of malabsorption, the significance of the fasting value itself is unknown²³. Long-term (six months) and daily inhalation of H_2 reduced the body weight and visceral fat volume compared to the control in rats^{24,25}. The decrease in the maximum performance of the skeletal muscle was significant at the beginning of the introduction of 3.1 MPa of H_2 into the breathing mixture, then returned to the control level at 0.9 MPa during decompression in humans²⁶. Excess H_2 may reduce body weight and muscular performance. However, in young and healthy people, H_2 inhalation improved running performance and torso strength²⁷. In other research, H_2 reduced delayed-onset muscle soreness after running downhill²⁸. These data suggest that little remains known about the proper range of H_2 through atmospheric, biological, and anthropogenic sources.

Breath H_2 excretion depends, not only on feeding and fasting patterns, but also on host organ functions¹⁴. Breath H_2 excretion is reduced by the consumption of a low-carbohydrate diet during the 24-h period preceding measurement and by fasting during the 12-h period preceding measurement²⁹. Resistant starch and dietary fibers have been shown to increase breath H_2 excretion, while cellulose reduces it^{30,31}. When breath H_2 tests were performed on subjects who consumed a stable diet, some variation in H_2 was observed³². High fasting breath H_2 was documented in patients with pancreatic exocrine insufficiency and those with small intestinal bacterial overgrowth^{33,34}. Low fasting H_2 concentrations have been reported in patients with congestive heart failure and those with Parkinson's disease^{35,36}. Elderly women show lower baseline and peak H_2 concentrations than young women³⁷. In this study, a meal consuming within 2 h before measurement (breakfast) did not have any influence on the end-tidal H_2 at baseline.

There was a clear circadian pattern of breath H_2 , high in the morning, decreasing to the nadir by 16:00, increasing again during the night in young women^{38,39}. The average profile of breath H_2 excretion during prolonged exercise was similar to that observed during the control study, in which each participant sat on a chair and lay down⁴⁰. In individuals with baseline H_2 levels above cutoff (20 ppm), new samples were taken after a 1-h light walk. The decrease in H_2 levels at 8 ppm and the influence of time of day, before or after 10:00 a.m., may be related⁴¹. Some of the young female students showed a bimodal pattern of breath H_2 excretion, high in the morning and decreasing later in the day, then increasing early in the afternoon and later decreasing. This was probably caused by the malabsorption of breakfast⁴². In this study, some of the subjects who ate breakfast showed increased H_2 excretion at noon. Changes in end-tidal H_2 after daily activities could be counteracted by consuming a meal 4–6 h before measurement (breakfast). It is suggested that end-tidal H_2 might follow either a circadian pattern or bimodal pattern.

H_2 is not directly involved in cellular metabolism, and its transport has not been thoroughly investigated⁴³. Some of the H_2 produced by the microbiome is absorbed into the blood, and dissolved H_2 diffuses into the alveolar air according to the Bunsen absorption coefficient (1.8 mL of H_2 /100 mL of water at 1 bar) and the ventilation-perfusion ratio (1.35 ± 0.22), which is the ratio of alveolar air (ℓ) per blood (ℓ) in normal-weight individuals aged 25–34 years⁴⁴. As a result, the dissolved H_2 will be diluted approximately 75 times ($\frac{100}{1.8} \times 1.35$) in the gas phase. The human lung has reciprocating ventilation with large terminal air space (alveoli). The volume of alveolar replaced by new atmospheric air is only one-seventh of the total (350 mL of alveolar ventilation/2300 mL of functional residual capacity)¹⁸. The slow replacement of alveolar air is of particular importance in preventing sudden changes in the concentration of gases like O_2 and CO_2 in the blood. The H_2 of alveolar gas equilibrates arterial blood during gas exchange. Extracellular fluids and tissues are saturated by H_2 in arterial blood. H_2 remains in the tissues until the H_2 partial pressure in the lungs drops below that of the relevant tissues⁴⁵.

The concentration of dissolved H_2 at the baseline (1.3 Pa = 1.3×10^{-5} bar) was estimated to be 10.1×10^{-9} M (10.1 nM) using Henry's law constants, as follows: $H^{cp} = 7.8 \times 10^{-4} \left(\frac{\text{mol}}{\text{L bar}} \right)^{46}$. The concentration of dissolved H_2 was similar to the arterial H^+ concentration at pH = 7.4, which is converted as $10^{-7.4} = 39 \times 10^{-9}$ M (39 nM). In this study, 10 mM of phosphate-buffered solution ($H_2PO_4^- \rightleftharpoons H^+ + HPO_4^{2-}$) was alkalizing (pH = 7.18 after air-bubbling with H_2 and pH = 7.08 after air bubbling without H_2). In the 1960s, Japan's health authorities endorsed the alkaline water ionizer as a medical device capable of producing both alkaline and acidic water. Alkaline ionized water and electrolyzed reduced water have alkaline pHs and high concentrations of dissolved H_2 . Drinking dissolved H_2 caused serum alkalization in the healthy human volunteers⁴⁷. Dissolved H_2 does not directly affect the pH of a solution ($2H^+ + 2e^- \rightleftharpoons H_2$). However, dissolved H_2 in the solution may influence pH measurement because uncertainty budget for the standard potential of the Ag|AgCl electrode includes $\log\left(\frac{p_{H_2}}{p^0}\right)^{22}$.

Under normobaric conditions, p_{H_2} ranges from 0 (1 bar of H_2 gas) to 6.2 (0.6 ppm of H_2 in the air). In this study, the median p_{H_2} at baseline was 4.89 and the 25th–75th percentile range of p_{H_2} was 4.59–5.30, which is broader than the normal pH range of 0.1. The electrode potential of a H^+/H_2 pair can be calculated using p_{H_2} and pH as $E \approx 30.8 \times (p_{H_2} - 2 \times pH)(\text{mV})$ at 37 °C. When local blood flow is measured in vivo, the current between a calomel half-cell and a platinum electrode in the tissue is proportional to the H_2 level⁴⁸. The p_{H_2} scale could serve as a measure of how reduced or oxidized water is wherever redox environment is common, given that pH is a measure of how acidic or basic water is⁴⁹.

To gain a more differentiated understanding of cellular redox biology, quantitative, redox-couple specific, in vivo measurements are necessary⁵⁰. Plasma cysteine/cystine and GSH/GSSG are oxidized at different rates as a function of age⁵¹. Those redox states undergo diurnal variation, and the mean differences between maximal and minimal redox state values for cysteine/cystine and GSH/GSSG were 6 and 4.5 mV, respectively, in 63 samples of healthy human plasma⁵². In the context of redox-sensitive proteins, a 6-mV difference is equivalent to a 1.6-fold increase in the ratio of dithiol to disulfide forms. However, in vitro studies have shown that variation in cysteine/cystine redox over the range found in vivo affects signaling pathways that control cell proliferation and oxidant-induced apoptosis⁵³. Moreover, 1.3–5.0% H_2 regulates various signal transduction pathways and the expression of many genes in human monocytic cell line⁵⁴. Hepatic oxidoreduction-related genes are upregulated by the administration of 0.7 mM- H_2 drinking water in rats⁵⁵. Recently, it has been reported that all collaborating metabolic organs can be regulated through changes in circulating redox metabolites regardless of whether the change was initiated exogenously or by a single organ⁵⁶. In this study, the variation of electrode potential was estimated to be 4.6 mV between before and after daily activities. It is rational to measure p_{H_2} as an electrode potential indicator that predicts organ functions and signaling pathway in vivo.

We acknowledge that while this investigation offers insight into a novel description of electrode potential variation in humans, there are limitations to this technology that must be overcome before it can be validated. H_2 is not a metabolite of human cells but instead an environmental factor that acts through H_2 -producing microbiomes. Intracellular electrode potential depends on the oxidized/reduced forms of metabolites in each intracellular compartment. The extracellular electrode potential affects the intracellular electrode potential, and the electrode potential depends on environmental factors such as O_2 and H_2 . The electrode potential is heavily influenced by 21% O_2 in the atmosphere and by less than 20 ppm of H_2 in the alveolar air under normoxia. This investigation provides the use of real-time, non-invasive means of estimating the variation of electrode potentials in healthy humans.

Materials and methods

Oxidation–reduction potential experiments. The effect of H_2 at low partial pressure was evaluated using the ORP of a phosphate buffer solution (10 mM at pH = 7.1; Fujifilm Wako Pure Chemical Corp., Osaka, Japan). For a mixture of gases at low pressure, the activity is equal to the ratio of the partial pressure of the gas over the standard pressure. The standard H_2 gas contains 100 ppm of H_2 (1×10^{-4} bar) in medical air, and the air contains 0.6 ppm of H_2 (0.6×10^{-6} bar). The phosphate-buffered solution was not aerated before the experiment, although tap water has a positive ORP ranging from +200 to +400 mV due to dissolved O_2 . The air was bubbled in a phosphate-buffered solution at a rate of 0.5 L/min using a humidifier water bottle for 60 min at 22 °C. The air was supplied from the integrated piping system at the TMG Asaka Medical Center (Air Water Inc., Osaka, Japan), and standard H_2 gas for calibration (100 ppm of H_2 in medical air; Air Water Inc., Osaka, Japan) was supplied from the cylinder with a pressure regulator. The ORP and pH were measured before and after the air bubbling using an ORP/pH meter (pH6600 and ORP6600S; Custom, Tokyo, Japan).

Clinical study. *Study design.* This was a non-randomized, non-blinded, prospective observational study performed to evaluate the variation of electrode potential using end-tidal H_2 levels in healthy Japanese subjects. This study's protocol was approved by the ethical review board of TMG Asaka Medical Center. The trial (UMIN000014696) was registered in the University Hospital Medical Information Network in Japan in May 2018. All participants provided written informed consent before enrollment. The study was performed between September 2018 and December 2018 at the TMG Asaka Medical Center in Saitama.

Participants. We enrolled 160 healthy, non-obese Japanese subjects (BMI < 30). We then excluded 11 smokers. Of the remaining 149 subjects, 98 were women and 51 were men, with an average age of 29.8 ± 9.0 years. All methods were performed in accordance with the relevant guidelines and regulations²⁸. In this study, H_2 concentration was measured using a portable handheld H_2 breath test apparatus (Gastrolyser; Bedfont Scientific Ltd.,

Kent, UK) after 15 s of breath-holding^{57,58}. The time point at which the concentration of H₂ in the breath equilibrated or flattened to that in the blood was 15–20 s. Then, subjects were asked to exhale slowly but gently into the mouthpiece, aiming to empty their lungs completely for accurate breath analysis with end-tidal samples⁵⁹. Measurements taken at 8:00 a.m. served as the baseline. The subjects were then allowed to start their daily activities, which included in-hospital desk and laboratory work as well as physical therapy. Measurements were taken again after daily activities at noon but before lunch to prevent eating and drinking from influencing the breath test results. Calibration was performed using standard H₂ gas (100 ppm of H₂ gas in medical air, 0.5 L/min of flow) as 100 ppm, and the atmospheric pressure was set to 0 points. The end-tidal H₂ partial pressure was calculated as follows: $P = (H_2 \text{ concentration}) \times 100 \text{ kPa}$ or 0.06 Pa at 0 points of H₂ concentration. End-tidal hydrogen levels were measured by a hand-held electrochemical H₂ sensor. Electrochemical gas sensors have become popular due to their linearity of output. In addition, once the correction is performed with a known concentration of the target gas, it provides excellent repeatability and accuracy during measurements. Technological advances over the past few decades have enabled electrochemical gas sensors to show very good selectivity for specific gas types. In addition, although selectivity for the target gas has been greatly improved, the cross-sensitivity to other gases is still not zero, increasing the possibility of interference and misdirection during measurements. The detection range of the H₂ sensor is 0–500 ppm. The accuracy is $\pm 10\%$ and CO cross interference is less than 1%. Accurate measurement of H₂ in ppm in expiratory air reveals intolerance and/or malabsorption of carbohydrates; or bacterial over growth.

Before testing, all subjects answered a questionnaire covering meals, exercise habits, and bowel movements.

Statistical analyses. All statistical analyses were performed using IBM SPSS Statistics, version 25 (IBM Corp., Armonk, NY, USA). Values of pH₂ are presented as medians and interquartile ranges. The univariate analysis was generally based on non-parametric methods (Wilcoxon or Mann–Whitney *U*). $P < 0.05$ was considered statistically significant.

Data availability

The datasets used and/or analyzed during the current study are available from the corresponding author upon reasonable request.

Received: 17 February 2023; Accepted: 13 September 2023

Published online: 19 September 2023

References

- Greening, C., Islam, Z. F. & Bay, S. K. Hydrogen is a major lifeline for aerobic bacteria. *Trends Microbiol.* **30**, 330–337 (2022).
- Berney, M., Greening, C., Conrad, R., Jacobs, W. R. J. & Cook, G. M. An obligately aerobic soil bacterium activates fermentative hydrogen production to survive reductive stress during hypoxia. *Proc. Natl. Acad. Sci. U S A.* **111**, 11479–21184 (2014).
- Wolf, P. G., Biswas, A., Morales, S. E., Greening, C. & Gaskins, H. R. H₂ metabolism is widespread and diverse among human colonic microbes. *Gut Microbes.* **7**, 235–245 (2016).
- Ohsawa, I. *et al.* Hydrogen acts as a therapeutic antioxidant by selectively reducing cytotoxic oxygen radicals. *Nat. Med.* **13**, 688–694 (2007).
- Nakai, Y. *et al.* Hepatic oxidoreduction-related genes are upregulated by administration of hydrogen-saturated drinking water. *Biosci. Biotechnol. Biochem.* **75**, 774–776 (2011).
- Benoit, S. L., Maier, R. J., Sawers, R. G. & Greening, C. Molecular hydrogen metabolism: A widespread trait of pathogenic bacteria and protists. *Microbiol. Mol. Biol. Rev.* **84**, e0009219. <https://doi.org/10.1128/MMBR.00092-19> (2020).
- Hammer, H. F. Colonic hydrogen absorption: Quantification of its effect on hydrogen accumulation caused by bacterial fermentation of carbohydrates. *Gut* **34**, 818–822 (1993).
- Baker, A. B. & Farmery, A. D. Inert gas transport in blood and tissues. *Compr. Physiol.* **1**, 569–592 (2011).
- Yamamoto, R., Homma, K., Suzuki, S., Sano, M. & Sasaki, J. Hydrogen gas distribution in organs after inhalation: Real-time monitoring of tissue hydrogen concentration in rat. *Sci. Rep.* **9**, 1255. <https://doi.org/10.1038/s41598-018-38180-4> (2019).
- Machens, H. G. *et al.* Postoperative blood flow monitoring after free-tissue transfer by means of the hydrogen clearance technique. *Plast. Reconstr. Surg.* **99**, 493–505 (1997).
- Ketty, S. S. The theory and applications of the exchange of inert gas at the lungs and tissues. *Pharmacol. Rev.* **3**, 1–41 (1951).
- Levitt, M. D. & Donaldson, R. M. Use of respiratory hydrogen (H₂) excretion to detect carbohydrate malabsorption. *J. Lab. Clin. Med.* **75**, 937–945 (1970).
- Metz, G., Gassull, M. A., Leeds, A. R., Blendis, L. M. & Jenkins, D. J. A simple method of measuring breath hydrogen in carbohydrate malabsorption by end-expiratory sampling. *Clin. Sci. Mol. Med.* **50**, 237–240 (1976).
- Gasbarrini, A. *et al.* Methodology and indications of H₂-breath testing in gastrointestinal diseases: The Rome Consensus Conference. *Aliment. Pharmacol. Ther.* **29**, 1–49 (2009).
- Rezaie, A. *et al.* Hydrogen and methane-based breath testing in gastrointestinal disorders: The North American Consensus. *Am. J. Gastroenterol.* **112**, 775–884 (2017).
- Hammer, H. F. *et al.* European guideline on indications, performance, and clinical impact of hydrogen and methane breath tests in adult and pediatric patients: European Association for Gastroenterology, Endoscopy and Nutrition, European Society of Neurogastroenterology and Motility, and European Society for Paediatric Gastroenterology Hepatology and Nutrition consensus. *United Eur. Gastroenterol. J.* **10**, 15–40 (2022).
- Jerkiewicz, G. Standard and reversible hydrogen electrodes: Theory, design, operation, and applications. *ACS Catal.* **10**, 8409–8417 (2020).
- Hall, J. E. Physical principles of gas exchange. In *Guyton and hall textbook of medical physiology* (12th ed) 485–494 (WB Saunders, 2015).
- Schafer, F. Q. & Buettner, G. R. Redox environment of the cell as viewed through the redox state of the glutathione disulfide/glutathione couple. *Free Radic. Biol. Med.* **30**, 1191–1212 (2001).
- George, S. M., Richardson, L. C., Pol, I. E. & Peck, M. W. Effect of oxygen concentration and redox potential on recovery of sublethally heat-damaged cells of *Escherichia coli* O157:H7, *Salmonella enteritidis* and *Listeria monocytogenes*. *J. Appl. Microbiol.* **84**, 903–909 (1998).

21. Matsumoto, K., Miyazaki, K., Hwang, J., Yamamoto, T. & Sakuda, A. Electrode potentials part 1: Fundamentals and aqueous systems. *Electrochemistry* **90**, 120201. <https://doi.org/10.5796/electrochemistry.22-66075> (2022).
22. Buck, R. P. *et al.* Measurement of pH definition, standards, and procedures. *Pure Appl. Chem.* **74**, 2169–2200 (2002).
23. Perman, J. A., Modler, S., Barr, R. G. & Rosenthal, P. Fasting breath hydrogen concentration: Normal values and clinical application. *Gastroenterology* **87**, 1358–1363 (1984).
24. Adzavon, Y. M. *et al.* Long-term and daily use of molecular hydrogen induces reprogramming of liver metabolism in rats by modulating NADP/NADPH redox pathways. *Sci. Rep.* **12**, 3904. <https://doi.org/10.1038/s41598-022-07710-6> (2022).
25. Xun, Z. *et al.* Effects of long-term hydrogen intervention on the physiological function of rats. *Sci. Rep.* **10**, 18509. <https://doi.org/10.1038/s41598-020-75492-w> (2020).
26. Fontanari, P. *et al.* Changes in maximal performance of inspiratory and skeletal muscles during and after the 7.1-MPa Hydra 10 record human dive. *Eur. J. Appl. Physiol.* **81**, 325–328 (2000).
27. Javorac, D., Stajer, V., Ratgeber, L., Betlehem, J. & Ostojic, S. Short-term H₂ inhalation improves running performance and torso strength in healthy adults. *Biol. Sport.* **36**, 333–339 (2019).
28. Kawamura, T. *et al.* Involvement of neutrophil dynamics and function in exercise-induced muscle damage and delayed-onset muscle soreness: Effect of hydrogen bath. *Antioxid. Basel* **7**, 127. <https://doi.org/10.3390/antiox7100127> (2018).
29. Avallone, E. V., De Carolis, A., Loizos, P., Corrado, C. & Vernia, P. Hydrogen breath test–diet and basal H₂ excretion: A technical note. *Digestion* **82**, 39–41 (2010).
30. van Munster, I. P. *et al.* Effect of resistant starch on breath-hydrogen and methane excretion in healthy volunteers. *Am. J. Clin. Nutr.* **59**, 626–630 (1994).
31. Nagano, A. *et al.* Effects of different types of dietary fibers on fermentation by intestinal flora, Hiroshima. *J. Med. Sci.* **67**, 1–5 (2018).
32. Yao, C. K. *et al.* Poor reproducibility of breath hydrogen testing: Implications for its application in functional bowel disorders. *United Eur. Gastroenterol. J.* **5**, 284–292 (2017).
33. Uetsuki, K. *et al.* Measurement of fasting breath hydrogen concentration as a simple diagnostic method for pancreatic exocrine insufficiency. *BMC Gastroenterol.* **21**, 211. <https://doi.org/10.1186/s12876-021-01776-8> (2021).
34. Takakura, W. & Pimentel, M. Small intestinal bacterial overgrowth and irritable bowel syndrome—an update. *Front. Psychiatry* **11**, 664. <https://doi.org/10.3389/fpsy.2020.00664> (2020).
35. Shibata, A. *et al.* Decrease in exhaled hydrogen as marker of congestive heart failure. *Open Heart.* **5**, e000814. <https://doi.org/10.1136/openhrt-2018-000814> (2018).
36. Suzuki, A. *et al.* Quantification of hydrogen production by intestinal bacteria that are specifically dysregulated in Parkinson's disease. *PLoS ONE* **13**, e0208313. <https://doi.org/10.1371/journal.pone.0208313> (2018).
37. Kagaya, M., Iwata, N., Toda, Y., Nakae, Y. & Kondo, T. Small bowel transit time and colonic fermentation in young and elderly women. *J. Gastroenterol.* **32**, 453–456 (1997).
38. Kagaya, M., Iwata, M., Toda, Y., Nakae, Y. & Kondo, T. Circadian rhythm of breath hydrogen in young women. *J. Gastroenterol.* **33**, 472–476 (1998).
39. Le Marchand, L., Wilkens, L. R., Harwood, P. & Cooney, R. V. Use of breath hydrogen and methane as markers of colonic fermentation in epidemiologic studies: Circadian patterns of excretion. *Environ. Health Perspect.* **98**, 199–202 (1992).
40. Cammack, J., Read, N. W., Cann, P. A., Greenwood, B. & Holgate, A. M. Effect of prolonged exercise on the passage of a solid meal through the stomach and small intestine. *Gut* **23**, 957–961 (1982).
41. Alegre, E., Sandúa, A., Calleja, S., Deza, S. & González, Á. Modification of baseline status to improve breath tests performance. *Sci. Rep.* **12**, 9752. <https://doi.org/10.1038/s41598-022-14210-0> (2022).
42. Sone, Y. *et al.* Everyday breath hydrogen excretion profile in Japanese young female students. *J. Physiol. Anthropol. Appl. Hum. Sci.* **19**, 229–237 (2000).
43. Christl, S. U., Murgatroyd, P. R., Gibson, G. R. & Cummings, J. H. Production, metabolism, and excretion of hydrogen in the large intestine. *Gastroenterology* **102**, 1269–1277 (1992).
44. Brochu, P., Brodeur, J. & Krishnan, K. Derivation of cardiac output and alveolar ventilation rate based on energy expenditure measurements in healthy males and females. *J. Appl. Toxicol.* **32**, 564–580 (2012).
45. Cao, D., Ye, Z. & Liu, W. Absorption and release of hydrogen gas in body. In *Hydrogen Molecular Biology and Medicine* (eds. Sun, X. *et al.*) 25–34 (Springer, 2015).
46. Sander, R. Compilation of Henry's law constants (version 4.0) for water as solvent. *Atmos. Chem. Phys.* **15**, 4399–4981 (2015).
47. Ostojic, S. M. Serum alkalinization and hydrogen-rich water in healthy men. *Mayo Clin. Proc.* **87**, 501–502 (2012).
48. Aukland, K., Bower, B. F. & Berliner, R. W. Measurement of local blood flow with hydrogen gas. *Circ. Res.* **14**, 164–187 (1964).
49. Shapiro, H. M. Redox balance in the body: An approach to quantitation. *J. Surg. Res.* **13**, 138–152 (1972).
50. Morgan, B., Sobotta, M. C. & Dick, T. P. Measuring E_{GSH} and H₂O₂ with roGFP2-based redox probes. *Free Radic. Biol. Med.* **51**, 1943–1951 (2011).
51. Jones, D. P., Mody, V. C. Jr., Carlson, J. L., Lynn, M. J. & Sternberg, P. Jr. Redox analysis of human plasma allows separation of pro-oxidant events of aging from decline in antioxidant defenses. *Free Radic. Biol. Med.* **33**, 1290–1300 (2002).
52. Blanco, R. A. *et al.* Diurnal variation in glutathione and cysteine redox states in human plasma. *Am. J. Clin. Nutr.* **86**, 1016–1023 (2007).
53. Jones, D. P. Extracellular redox state: Refining the definition of oxidative stress in aging. *Rejuvenat. Res.* **9**, 169–181 (2006).
54. Iuchi, K. *et al.* Molecular hydrogen regulates gene expression by modifying the free radical chain reaction-dependent generation of oxidized phospholipid mediators. *Sci. Rep.* **6**, 18971. <https://doi.org/10.1038/srep18971> (2016).
55. Kajiya, M. *et al.* Hydrogen from intestinal bacteria is protective for Concanavalin A-induced hepatitis. *Biochem. Biophys. Res. Commun.* **386**, 16–21 (2009).
56. Corkey, B. E. & Deeney, J. T. The redox communication network as a regulator of metabolism. *Front. Physiol.* **11**, 567796. <https://doi.org/10.3389/fphys.2020.567796> (2020).
57. Pitcher, C. K., Farmer, A. D., Haworth, J. J., Treadway, S. & Hobson, A. R. Performance and interpretation of hydrogen and methane breath testing impact of North American Consensus guidelines. *Dig. Dis. Sci.* **67**, 5571–5579 (2022).
58. Fitriakusumah, Y. *et al.* The role of Small Intestinal Bacterial Overgrowth (SIBO) in Non-alcoholic Fatty Liver Disease (NAFLD) patients evaluated using Controlled Attenuation Parameter (CAP) Transient Elastography (TE): A tertiary referral center experience. *BMC Gastroenterol.* **19**, 43. <https://doi.org/10.1186/s12876-019-0960-x> (2019).
59. Lee, S. M., Falconer, I. H. E., Madden, T. & Laidler, P. O. Characteristics of oxygen concentration and the role of correction factor in real-time GI breath test. *BMJ Open Gastroenterol.* **8**, e000640. <https://doi.org/10.1136/bmjgast-2021-000640> (2021).

Acknowledgements

We thank LetPub (www.letpub.com) for linguistic assistance and pre-submission expert review.

Author contributions

T.K. performed the study and wrote the manuscript. All authors contributed to manuscript revision and have read and approved the submitted version.

Funding

The authors declare that the research was conducted in the absence of any commercial or financial relationships that could be construed as a potential conflict of interest. T.K. has filed a patent application for the technology described in this paper. This project did not receive any specific grant from funding agencies in the public, commercial, or not-for-profit sectors.

Competing interests

T.K. has filed a patent application for the technology described in this paper.

Additional information

Correspondence and requests for materials should be addressed to T.K.

Reprints and permissions information is available at www.nature.com/reprints.

Publisher's note Springer Nature remains neutral with regard to jurisdictional claims in published maps and institutional affiliations.



Open Access This article is licensed under a Creative Commons Attribution 4.0 International License, which permits use, sharing, adaptation, distribution and reproduction in any medium or format, as long as you give appropriate credit to the original author(s) and the source, provide a link to the Creative Commons licence, and indicate if changes were made. The images or other third party material in this article are included in the article's Creative Commons licence, unless indicated otherwise in a credit line to the material. If material is not included in the article's Creative Commons licence and your intended use is not permitted by statutory regulation or exceeds the permitted use, you will need to obtain permission directly from the copyright holder. To view a copy of this licence, visit <http://creativecommons.org/licenses/by/4.0/>.

© The Author(s) 2023